3-4 Generation and Application of Quantum-Correlated Twin Beams

KASAI Katsuyuki, ZHANG Yun, and SASAKI Masahide

The signal and idler beams from a non-degenerate, above threshold, optical parametric oscillator have a strong quantum correlation, which are called twin beams. This correlation arises from the simultaneous generation of the signal and idler photons in the form of twin pairs of photons through the parametric down conversion, and the generated twin beams have exactly the same photon statistics. As a result, the fluctuations on the difference between the intensities of the twin beams are reduced with respect to the shot-noise limit, that is, intensity-difference squeezing. We have observed squeezing of 8 dB (84%) on the intensity difference between the twin beams generated by a semimonolithic optical parametric oscillator. In this paper, a comprehensive overview of the generation of twin beams using the optical parametric oscillator and the applications exploiting the quantum correlation of twin beams are presented.

Keywords
Optical parametric oscillator, Quantum noise, Squeezing, Quantum correlation, Twin beams

1 Introduction

Along with increasing research and development in the field of quantum information science, techniques to generate light with controlled quantum states—such as squeezed light with suppressed quantum noise and light with quantum correlation—have become indispensable resources[1]. Through the government-supported projects entitled "The Frontier of Telecommunications Technology" and "Basic Research 21 for Breakthroughs in Info-Communications," we have conducted research on the generation of two types of continuous-wave (CW) squeezed light: squeezed vacuum fields using a degenerate optical parametric oscillator [2]-[4], and bright squeezed light using cascading nonlinearity in an optical parametric oscillator [5]-[10]. Examples of the generation of squeezed light in various countries are summarized in the table in Reference [11]. Based on these studies, we conducted research on the generation and application of quantum-correlated twin beams using optical parametric oscillators. In an optical parametric oscillator, the optical parametric process causes strong quantum correlation between the modes of the signal field and the idler field. In a non-degenerate optical parametric oscillator, the generated signal and idler beams have different polarization or frequency values, which makes it possible to separate these beams. In this case, the fluctuations in the intensity difference between the two beams is below the quantum noise limit; the two beams are thus designated as quantum-correlated twin beams. In other words, we obtain squeezing in the intensity difference owing to the non-classical correlation between the twin beams. With quantum-correlated twin beams, we can extract information embedded below the quantum noise level in one of the beams by referring to the other beam. This characteristic is expected to develop into application technologies involving, for example, embedding of the hidden message within quantum noise or sub-shot-noise high-sensitivity measurement.

This paper reports on the principles and experimental results relating to the generation of quantum-correlated twin beams using a CW non-degenerate optical parametric oscillator.

2 Principles of generation of quantum-correlated twin beams

Here we will discuss the principles behind the generation of quantum-correlated twin beams using an optical parametric oscillator. According to the particle model of quantum theory, light can be treated as discrete photons, and a coherent laser beam can be viewed as a beam comprised of a series of photons. These photons obey a stochastic process referred to as the Poisson process. According to this process, the detector receives a photon randomly, and it cannot be known exactly when the detector will receive the next photon. The shot noise observed in the photodetector is due to this randomness in the photon series, and corresponds to the magnitude of the quantum noise in the coherent light. When a half beamsplitter divides the light beam (consisting of the photon series) into two beams, each photon will pass through either of the output ports of the beamsplitter randomly, with a probability of 1/2, as a photon cannot be divided in two. Each of the divided beams holds the same average number of photons, but as shown in Fig. 1 (a), these photons are randomly aligned along the time axis. The shot noise observed at each detector is due to the randomness in the photon series. As there is no correlation between the two shot noises at the respective detectors, these quantities do not cancel out; one cannot simply be subtracted from the other. On the other hand, in the optical parametric process, the input pump beam consists of a random series of photons, but the process transforms each photon into two photons (under the law of conservation of energy), providing the functions of a parametric beam splitter. A pump beam with an angular frequency of ω_0 is converted into a signal beam with a frequency of ω_1 and an idler beam with a frequency of ω_2, where $\omega_0=\omega_1+\omega_2$. Here, the photons of the signal and idler beams are generated simultaneously as a photon pair in the two optical paths (See Fig.1(b)). The two beams consist of photons with the same timing, and the photons enter the detectors simultaneously. When one of the detectors receives a photon, the other also receives a photon. Here, a correlation is obtained between the shot noises observed in the two detectors due to the randomness in the photon series, and these shot noises cancel each other out by subtraction. The photon pair exists simultaneously due to the quantum correlation—a phenomenon that cannot be explained classically. The noise in the intensity difference between the beams (consisting of paired photons sharing the same timing) is thus suppressed below the shot-noise limit. This effect is known as the intensity-difference squeezing of quantum-correlated twin beams. When quantum-correlated twin beams are generated with an optical parametric oscillator, the photon pair simultaneously generat-

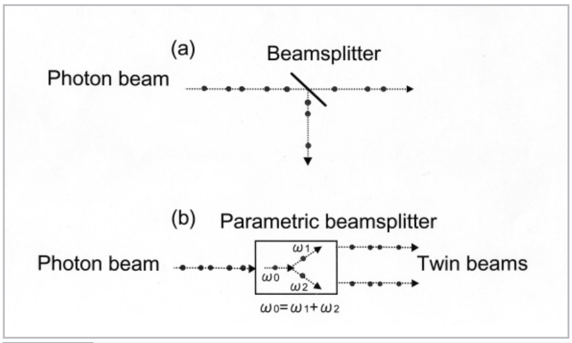

Fig.1 *(a) Beamsplitter and (b) parametric beamsplitter in photon picture.*

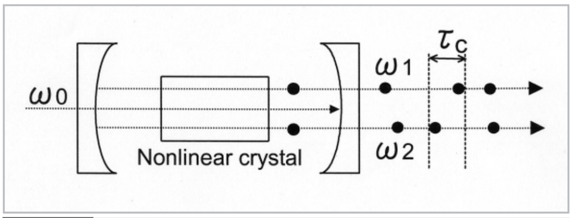

Fig.2 *Decorrelation of twin beams by cavity storage; τ_c is cavity storage time.*

ed in the nonlinear crystal remains in the cavity for an average storage time τ_c. Each of the photon pair is emitted from the cavity through independent stochastic processes, but the photon numbers of the signal and idler beams are the same if observed for a period longer than the average storage time τ_c (See Fig. 2). In other words, the twin beams generated from the optical parametric oscillator feature a quantum correlation within the bandwidth of the cavity, τ_c^{-1} [12].

3 Calculation of squeezing using a semi-classical approach

In the previous section we described the concepts behind the generation of quantum-correlated twin beams from an optical parametric oscillator, applying an interpretation of photons based on the particle model of light. Another interpretation is also possible. For example, in Fig. 1 (a), the correlation between the two output ports can be interpreted to be broken due to the vacuum fluctuations entering from the empty port of the beam splitter. In this case, the uncertainty principle is seen as the cause of the vacuum fluctuations. However, once the existence of these fluctuations is acknowledged, a classical treatment may be applied to the remaining analysis. Such a semi-classical approach is also extremely effective when considering the optical parametric oscillator, as this approach simplifies the theoretical treatment of this device [13][14]. In an optical parametric oscillator, the vacuum field can be considered to enter through the losses in the coupling mirror and the crystal. Denoting the complex amplitude of the electric fields inside the cavity as α_1 (signal field), α_2 (idler field), and α_0 (pump field), the time evolution of the signal and idler fields are related in accordance with the following basic equations for the parametric interaction:

$$\tau\dot{\alpha}_1 = -\gamma_1'\alpha_1 + 2\chi\alpha_0\alpha_2^* + \sqrt{2\gamma_1}\alpha_1^{in} + \sqrt{2\mu_1}\beta_1^{in}, \tag{1a}$$

$$\tau\dot{\alpha}_2 = -\gamma_2'\alpha_2 + 2\chi\alpha_0\alpha_1^* + \sqrt{2\gamma_2}\alpha_2^{in} + \sqrt{2\mu_2}\beta_2^{in}. \tag{1b}$$

Here, the relationship $\gamma_i' = \gamma_i + \mu_i$ (i=1,2) holds, where γ_i is the loss factor of the coupling mirror of the cavity, μ_i is the loss factor inside the cavity due to crystals and other elements, τ is the round-trip time in the cavity, and χ is a constant representing the strength of the parametric interaction and is proportional to the second-order non-linear optical coefficient. Denoting the reflection coefficient of the cavity output mirror as r_i and the amplitude transmission coefficient as t_i, these can be expressed as follows in a high-finesse ($r \approx 1$) cavity:

$$r_i = 1 - \gamma_i \quad , \quad t_i = (2\gamma_i)^{1/2}. \tag{2}$$

Here, α_i^{in} and β_i^{in} (i=1,2) represent vacuum fields which have zero mean values, due to coupling mirror loss and loss inside the cavity. Output α_i^{out} through the coupling mirror is related to α_i inside the cavity by the following equation:

$$\alpha_i^{out} = t_i\alpha_i - \alpha_i^{in}. \tag{3}$$

Expanding Equation (1) with fluctuations $\delta\alpha_i$ around the steady-state solution, α_i is expressed as $\alpha_i = \overline{\alpha_i} + \delta\alpha_i$. The steady-state solution $\overline{\alpha_0}$ is assumed to be real. As the phase is arbitrary in Equation (1), which expresses the parametric interaction, $\overline{\alpha_1}$ and $\overline{\alpha_2}$ are also assumed to be real. The differential equations for the fluctuations are then expressed as follows:

$$\tau\delta\dot{\alpha}_1 = -\gamma_1'\delta\alpha_1 + 2\chi\overline{\alpha}_0\delta\alpha_2^* + 2\chi\overline{\alpha}_2\delta\alpha_0 + \sqrt{2\gamma_1}\delta\alpha_1^{in} + \sqrt{2\mu_1}\delta\beta_1^{in}, \tag{4a}$$

$$\tau\delta\dot{\alpha}_2 = -\gamma_2'\delta\alpha_2 + 2\chi\overline{\alpha}_0\delta\alpha_1^* + 2\chi\overline{\alpha}_1\delta\alpha_0 + \sqrt{2\gamma_2}\delta\alpha_2^{in} + \sqrt{2\mu_2}\delta\beta_2^{in}. \tag{4b}$$

Here we consider the case $I_1^{out} = I_2^{out} = I^{out}$, in which the signal and idler beam intensities are in balance. In this case, the following relationships hold:

$$\gamma_1 = \gamma_2 = \gamma \ , \ \mu_1 = \mu_2 = \mu \ , \ \gamma_1' = \gamma_2' = \gamma', \tag{5}$$

$$\overline{\alpha}_1 = \overline{\alpha}_2 \ , \ \overline{\alpha}_1^{out} = \overline{\alpha}_2^{out}. \tag{6}$$

From Equation (1), the steady-state solution for α_0 above the oscillation threshold is:

$$\overline{\alpha_0} = \frac{\sqrt{\gamma_1'\gamma_2'}}{2\chi} = \frac{\gamma'}{2\chi}. \tag{7}$$

Under these conditions, the difference in the fluctuations of the signal and idler fields is proportional to the real part of the difference between $\delta\alpha_1$ and $\delta\alpha_2$. Here, we denote

$$r = \sqrt{2}\,\mathrm{Re}(\delta\alpha_1 - \delta\alpha_2), \tag{8}$$

and express the entering vacuum fluctuations as r_α^{in} and r_β^{in} in a similar manner. With Equations (4) and (7), the following equation is obtained regarding *r*.

$$\tau\dot{r} = -2\gamma' r + \sqrt{2\gamma}\, r_\alpha^{in} + \sqrt{2\mu}\, r_\beta^{in}. \tag{9}$$

When the two fields are balanced, subtraction cancels out pump fluctuations $\delta\alpha_0$. Thus, in principle, intensity-difference squeezing of twin beams in a balanced system has robust characteristics in terms of the pump fluctuations. Taking the Fourier transformation of Equation (9),

$$\tilde{r}(\omega) = \frac{1}{2\gamma' + i\omega\tau}\left[\sqrt{2\gamma}\,\tilde{r}_\alpha^{in}(\omega) + \sqrt{2\mu}\,\tilde{r}_\beta^{in}(\omega)\right] \tag{10}$$

is obtained. The output from the cavity, r^{out}, is expressed as follows, derived from a relation similar to Equation (3):

$$\tilde{r}^{out}(\omega) = -\frac{i\omega\tau + 2\mu}{i\omega\tau + 2\gamma'}\tilde{r}_\alpha^{in}(\omega) + \frac{2\sqrt{\gamma\mu}}{i\omega\tau + 2\gamma'}\tilde{r}_\beta^{in}(\omega). \tag{11}$$

Here, $r_\alpha^{in}(\omega)$ and $r_\beta^{in}(\omega)$ are the vacuum fluctuations; these values are uncorrelated. Denoting the variance of the fluctuations as

$$\left\langle \left|\tilde{r}_\alpha^{in}(\omega)\right|^2 \right\rangle = \left\langle \left|\tilde{r}_\beta^{in}(\omega)\right|^2 \right\rangle = V_r^{in}, \tag{12}$$

the following expression is obtained:

$$\left\langle \left|\tilde{r}^{out}(\omega)\right|^2 \right\rangle = \left(\left|\frac{i\omega\tau + 2\mu}{i\omega\tau + 2\gamma'}\right|^2 + \frac{4\gamma\mu}{\left|i\omega\tau + 2\gamma'\right|^2} \right) V_r^{in}$$
$$= \left(\frac{\omega^2\tau^2 + 4\mu\gamma'}{\omega^2\tau^2 + 4\gamma'^2} \right) V_r^{in}. \tag{13}$$

The fluctuations $\delta\tilde{I}^{out}(\omega)$ of the intensity difference is expressed as

$$\delta\tilde{I}^{out}(\omega) = \sqrt{2}\,\bar{\alpha}_1^{out}\,\tilde{r}^{out}(\omega), \tag{14}$$

and the intensity-difference squeezing spectrum $S_I(\omega)$ of the twin beams is expressed as

$$S_I(\omega) = \left\langle \left|\delta\tilde{I}^{out}(\omega)\right|^2 \right\rangle = 2I^{out}\left\langle \left|\tilde{r}^{out}(\omega)\right|^2 \right\rangle \tag{15}$$
$$= \left(\frac{\omega^2\tau^2 + 4\mu\gamma'}{\omega^2\tau^2 + 4\gamma'^2} \right) S_0,$$

$$S_0 = 2I^{out}V_r^{in}. \tag{16}$$

The value S_0 in the above equation represents the shot-noise level of the twin beams. Denoting the efficiency of the detection system as η, and normalizing $S_I(\omega)$ with the shot-noise level, the squeezing spectrum (15) is rewritten as follows:

$$S(\Omega) = 1 - \frac{\eta\xi}{\Omega^2 + 1}. \tag{17}$$

Here, Ω is ω normalized with the full bandwidth at half maximum of the cavity, $\tau_c^{-1} = 2\gamma'/\tau$, and $\xi = \gamma/\gamma'$ is the escape efficiency. Figure 3 shows the squeezing spectrum $S(\Omega)$ as a function of Ω and the loss parameter ($1-\xi$) for the case in which detection efficiency is 100%. Here the magnitude of squeezing is denoted as $1-S(\Omega)$. Under ideal conditions, with no loss inside the cavity ($\xi = 1$), complete squeezing (100%) is obtained at Ω=0.

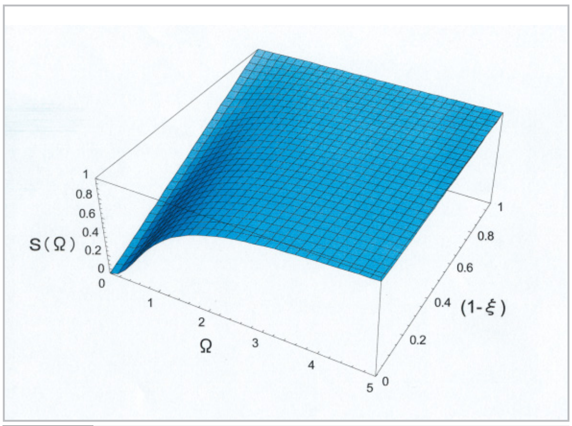

Fig.3 *Normalized noise spectrum $S(\Omega)$ of intensity-difference squeezing as a function of the loss parameter ($1-\xi$).*

4 Generation of twin beams and observation of the quantum correlation

The generation of quantum-correlated twin beams requires an optical parametric oscillator in which the signal and idler modes resonate. However, the resonance conditions of both modes must be satisfied, which renders CW oscillation extremely difficult [15]. Experiments in the past applied external stabilizing controls, such as feedback, to enable the generation of twin beams. In our case we successfully generated twin beams in the free running condition using a highly stable semimonolithic structure and applying thermal self-locking within a nonlinear crystal [10][16]. Here we discuss the results of our experiment in which twin beams are generated using a semimonolithic optical parametric oscillator. The experiment measures intensity difference squeezing in the presence of a quantum correlation and the non-classical photon number distribution between the twin beams [17]-[19].

Figure 4 shows the experimental setup for the generation of the twin beams and observation of intensity difference squeezing. For the pump beam source, the second harmonic of the CW LD-pumped YAG laser oscillating in a single frequency is used. The semimonolithic optical parametric oscillator consists of a 10-mm KTP (TYPE II) nonlinear crystal and a concave mirror with a radius of curvature of 20 mm. The facet of incidence of the KTP crystal for the pump beam is provided with a reflective coating, and it forms a three-wave resonance optical parametric oscillator with the output concave mirror, resonating the pump, signal, and idler fields. This structure provides strong parametric interaction and a low oscillation threshold. The oscillation threshold depends on the configuration and condition of the optical cavity. In this experiment, the threshold value is around 6 mW. Output oscillation power is 30 mW for input-pump beam power of 40 mW, with a conversion efficiency of 65%.

It is known that the three-wave resonance

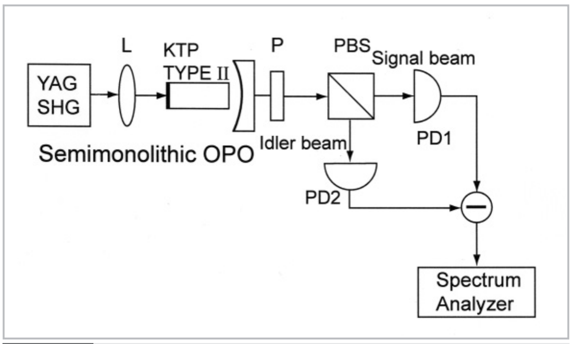

Fig.4 *Experimental setup for generation of twin beams (PD1, PD2: photodiodes, PBS: polarizing beamsplitter, P: half-wave plate, L: lens).*

optical parametric oscillator may produce the phenomenon of optical bistability, depending on the detuning condition of the cavity [6][20][21]. In the region of optical bistability, high finesse is obtained equivalently. This property is used to induce self-locking through the thermal effect in the crystal, and also sustain CW oscillation [22]. More than 30 minutes of stable optical parametric oscillation was obtained without feedback stability control of cavity length. As the quantum-correlated signal and idler beams feature orthogonal polarizations, these beams can be separated easily with the PBS. Figure 5 shows the results of noise observation of the intensity difference between the generated twin beams. The shot-noise level (a) is obtained by adjusting the $\lambda/2$ wave plate, P, in Fig. 4 to set the polarization of the beams to 45 degrees relative to the PBS. Here the PBS operates as a 50:50 beamsplitter for each photon beam. Thus the quantum correlation is broken without separation of the photon pair. As a result, observed noise gives the shot-noise level. The intensity difference squeezing (b) observed in the experiment shows a maximum value of 8 dB at a frequency of 4 MHz (84%). Considering the total detection efficiency, this indicates that squeezing of more than 90% is obtained. In this experiment, $\Omega \sim 0.06$ and $\xi \sim 0.95$. Applying the analysis results from the previous section, we may deduce that initial squeezing—just after the twin beams are generated from the cavity—is approximately 95%.

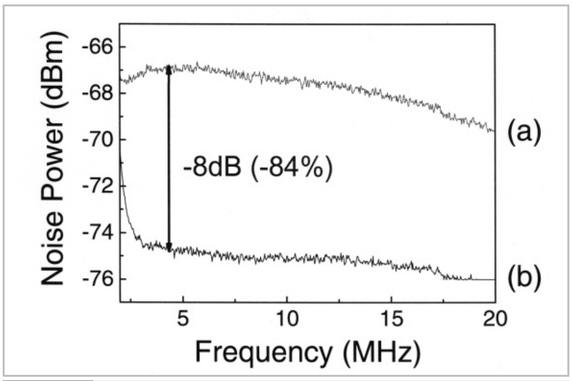

Fig.5 *Noise power spectrum of (a) the shot-noise level and (b) the intensity difference between twin beams.*

The fluctuations of the signal and idler beams, δI_1^{out} and δI_2^{out}, display a strong positive correlation exceeding the quantum limit. The joint probability distribution of the fluctuations between the two beams can be obtained by measuring the fluctuations of the photoelectric currents in the photodetectors directly and simultaneously [17][23]. As shown in Fig. 6, the photoelectric current noises of the signal and idler beams, directly detected by the photodetector D1 or D2, are passed through a lowpass filter, amplified by a low noise amplifier, electrically mixed with the local signal (4 MHz) for down conversion, simultaneously passed through another lowpass filter, AD converted, and input into a computer. Figure 7 (a) shows the joint probability distribution $P(X_A,X_B)$ obtained from the experiment, where X_A and X_B denote the 4-MHz signals of the detectors. Figure 7 (b) shows the joint probability distribution of the fluctuations obtained for two independent coherent beams (separable state) with the same mean intensity. A strong positive quantum correlation is observed in (a), while no correlation appears in (b).

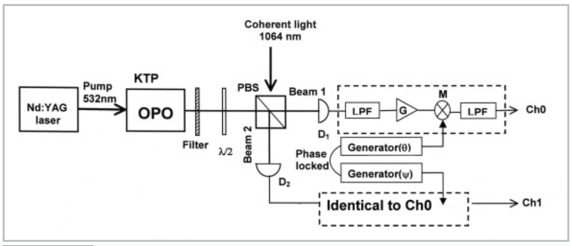

Fig.6 *Experimental setup for observation of the photon number distribution of twin beams.*

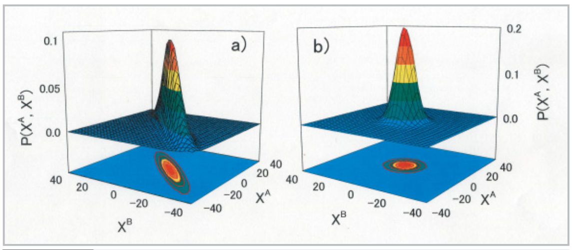

Fig.7 *Measured joint probability distribution for (a) twin beams and (b) separable state, viewed in 3D and as contour plots.*

The fluctuations in the intensity is in fact fluctuations of the photon number. When the quantum efficiency of the photodetectors is high, the probability distribution of the fluctuations in the photon-number difference between the twin beams can be obtained from the fluctuations of the photoelectric currents. Figure 8 shows the experimentally obtained probability distribution $P(n-m)$ of the fluctuations in photon-number difference between the beams. Here the mean photon numbers of the two beams are expressed as $\langle n \rangle \times 10^{15}$ and $\langle m \rangle \times 10^{15}$. For comparison, Fig.8 also shows the results for cases in which the polarizations of the twin beams are tilted 45 degrees relative to the PBS and where two independent coherent light beams are input to the detectors. It is clear that $P(n-m)$ of the twin beams obeys a sub-Poissonian distribution.

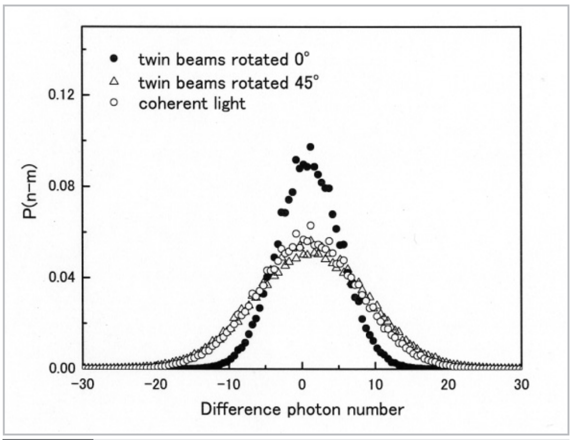

Fig.8 *Comparison of difference photon-number probability distribution P(n-m) on the condition of the same mean photon number.*

5 Applications

Quantum-correlated twin beams can be applied to spectroscopy, measurement, communications, and a range of other fields. High-sensitivity measurement and hidden-message embedding are two prime examples of such applications [24]-[29]. Here we present the results of basic experiments focusing on applications in the measurement of small magnetic fields below the shot-noise level and applications to the embedding of data within quantum noise [16][19][30].

5.1 Sub-shot-noise measurement

In an application for precision measurement technology, when a sensor element capable of changing polarization in response to the measurement target is inserted in one of the twin beams, it becomes possible to measure the change in polarization below the shot-noise level. Various physical quantities may form the measurement target. In this case, a change in polarization induced by a magnetic field is detected using the Faraday effect below the shot-noise level. Figure 9 shows the experimental setup. The Faraday glass (HOYA FR-5) is inserted in the signal beam and a small alternating magnetic field is applied (4 MHz). The polarizer PBSM converts the change in polarization into a small change in the intensity. The extremely small measurement signal embedded in the shot noise cannot be detected with conventional laser systems. However, quantum-correlated twin beams can cancel out the shot noise. Figure 10 shows the obtained experimental results. Figure 10 (a) is the shot-noise level, and (b) is the noise spectrum of the intensity difference between the twin beams. The magnetic signal below the shot-noise level is detected at a frequency of 4 MHz.

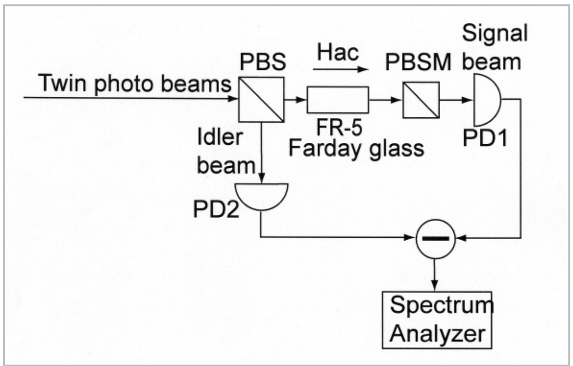

Fig.9 Experimental setup for sub-shot-noise measurement of AC magnetic field (PBS, PBSM: polarizing beamsplitters, PD1, PD2: photodiodes, Hac: magnetic field, FR-5: Faraday glass).

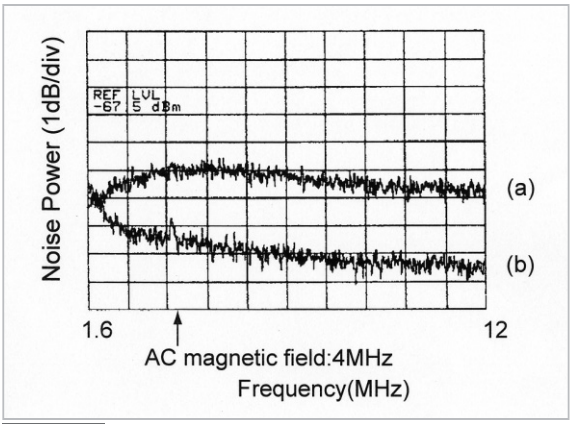

Fig.10 Experimental results of the detected magnetic field below the shot-noise level: (a) shot-noise level; (b) intensity-difference noise spectrum.

5.2 Quantum steganography

The use of quantum-correlated twin beams enables the recovery of the sub-shot-noise signal. In this case, messages can be imperceptibly embedded into background shot noise in optical communications. These messages can be conveyed via modulation of one of the twin beams below the shot-noise level, transmission of the signal, reception of the pairing photon beam, and cancellation of the shot noise. In other words, quantum noise conceals the message in a manner analogous to conventional steganography. Figure 11 shows the experimental setup. After the quantum-correlated twin beams are separated into the signal and idler beams with the PBS, an extremely weak modulation (at a frequency of 10 MHz) is applied to the signal beam below the shot-noise level with a light-intensity modulator comprised of a $LiNbO_3$ crystal and a polarizer. The weak signal is buried in the shot noise and can be extracted only by canceling out the shot noise with reference to the received pairing idler beam. In this experiment, quantum noise is canceled between the twin beams, allowing this property of quantum correlation to be applied to extract the weak modulation signal. The signal is mixed with a local oscillator for down conversion to 50 kHz, and the weak signal, below the shot-noise level, is observed with an oscilloscope. Figure 12 shows the results. Figure 12 (a) shows the condition in which the weak modulation signal is buried in the shot noise. In this case the signal cannot be identified. In Fig.12 (b), quantum noise is cancelled using the quantum correlation, and a weak signal—modulated below the shot-noise level—can be recognized.

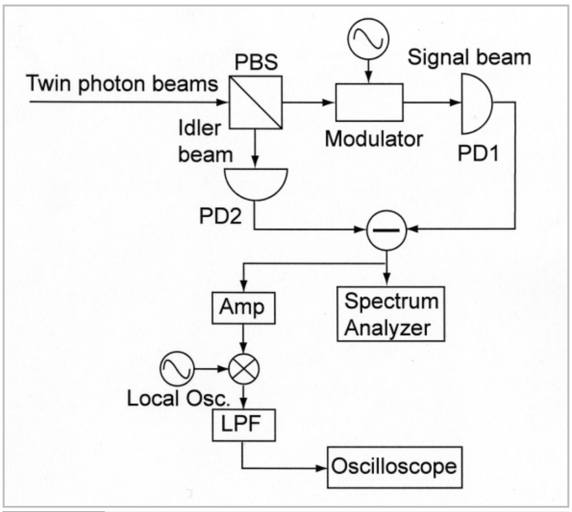

Fig.11 *Experimental setup for quantum steganographic application (PD1, PD2: photodiodes, PBS: polarizing beamsplitter, LPF: low-pass filter).*

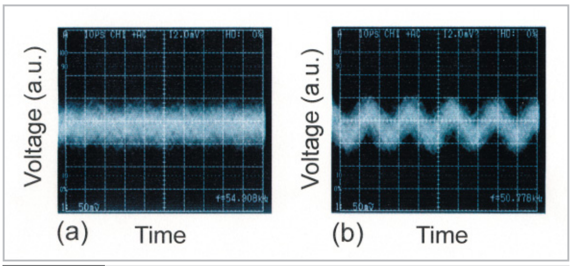

Fig.12 *Recovery of quantum steganographic signal (Time: 10 μsec/div). (a): The transmitted signal is hidden by the shot noise. (b): The transmitted signal is recovered by using twin beams.*

6 Summary

This paper discusses the principles of generation of quantum-correlated twin beams with an optical parametric oscillator, describes related experiments, and indicates some potential applications. The results of analysis under a semi-classical approach agree well with these experimental results; this type of analysis provides excellent results in terms of engineering system design. This analysis has led to the prediction that squeezing should be observed independently in the intensity of each of the quantum-correlated twin beams [14], and we are progressing with experiments to verify this theory [31]. In terms of applications, however, some issues remain to be addressed. For example, the wavelength of the twin beams needs to be continuously variable, as required in the field of spectroscopy [32][33].

Quantum-correlated twin beams will also prove advantageous in applications in which high-intensity light would damage the samples, for example in high-sensitivity biological measurement within living cells. Demand will also grow for the development of more compact light sources [34][35].

We intend to continue our research into the development of future quantum information and communications, and quantum measurement technologies, such as the generation and application of light featuring quantum correlation (EPR correlation) of quadrature components between light beams [36]-[40].

References

1 D. Bouwmeester, A. Ekert, A. Zeilinger (Eds.), The Physics of Quantum Information, Springer, 2000, and references therein.

2 K. Kasai and M. Ishizu, Jpn. J. Appl. Phys. 33, L230, 1994.

3 K. Kasai, Quantum Communications and Measurements, Plenum Press, 479,1995.

4 N. Onodera, M. Ishizu, K. Kasai, J. Zhou, M. Hyodo, M. Tani, and K. S. Abedin, Review of the Communications Research, Laboratory,Vol.43, No.4,611,1997. (in Japanese)

5 C. Fabre, C. Richy, and K. Kasai, Laser Phys. 6,339,1996.

6 K. Kasai and C. Fabre, J. Nonlin. Opt. Phys. Mater. 5,921,1996.

7 K. Kasai, G. Jiangrui, L.-A. Wu, and C. Fabre, Quantum Communication, Computing, and Measurements, Plenum Press, 439,1996.

8 K. Kasai, G. Jiangrui, L.-A. Wu, and C. Fabre, Frontiers of Quantum Optics and Laser Physics, Springer, 315, 1997.

9 K. Kasai, G. Jiangrui, and C. Fabre, Europhys. Lett. 40, 25, 1997.

10 K. Kasai, N. Onodera, J. Gao, C. Fabre, The Review of Laser Engineering, 28, 690, 2000(in Japanese).

11 Ed. T. Kushida, Laser Measurement, Maruzen Experimental Physics Lectures 9, 226, 2000(in Japanese).

12 S. Reynaud, Europhys. Lett. 4, 427, 1987.

13 S. Reynaud, C. Fabre, and E. Giacobino, J. Opt. Soc. Am. B4, 1520, 1987.

14 C. Fabre, E. Giacobino, A. Heidmann, and S. Reynaud, J. Phys. France 50, 1209, 1989.

15 R. G. Smith, Optical Parametric Oscillator in Laser Handbook I, Eds. F. Arecchi, E. Schulz-Dubois (North Holland Amsterdam), 1973.

16 K. Kasai and M. Watanabe, Proc.7th Int. Conf. on Squeezed States and Uncertainty Relations, Boston, 2001. Available at http://www.physics.umd.edu/rgroups/ep/yskim/boston/boston.html

17 Y. Zhang, K. Kasai, and M. Watanabe, Opt. Lett. 27, 1244, 2002.

18 Y. Zhang, K. Kasai, and M. Watanabe, Opt. Express 11, 14, 2003.

19 K. Kasai, Reports on the 307th Topical Meeting of The Laser Society of Japan, Lectures on 26th Prize of Laser Engineering, No. RTM-03-01, 2003. (In Japanese)

20 C. Fabre, C. Richy, and K. Kasai, Laser Phys. 6, 339, 1996.

21 C. Richy, K. Petsas, E. Giacobino, C. Fabre, and L. Lugiato, J. Opt. Soc. Am. B12, 456, 1995.

22 K. Kasai, Japan Patent 3421742, 2003.

23 K. Kasai, Y. Zhang, and M. Watanabe, The Sixth Quantum Information Technology Symposium, QIT2002-39, 2002(in Japanese).

24 C. Fabre, K. Kasai, J. Gao, C. Schwob, A. Maitre, and P. H. Souto-Ribeiro, Proc.5th Int. Conf. on Squeezed States and Uncertainty Relations, Balatonfured, Hungary, 1997.

25 P. H. Souto Ribeiro, C. Schwob, A. Maître, and C. Fabre, Opt. Lett. 22,1893,1997.

26 J. Gao, F. Cui, C. Xue, C. Xie, and P. Kunchi: Opt. Lett. 23, 870, 1998.

27 J. J. Snyder, E. Giacobino, C. Fabre, A. Heidmann, and M. Ducloy, J. Opt. Soc. Am. B7, 2132, 1990.

28 K. Kasai and Y. Zhang, The Seventh Quantum Information Technology Symposium, QIT2002-86, 2002. (in Japanese)

29 Y. Zhang, K. Kasai, and K. Hayasaka, Opt. Express 11, 3592, 2003.

30 K. Kasai, The Review of Laser Engineering, 31, 592, 2003. (in Japanese)

31 Y. Zhang, K. Kasai, and K. Hayasaka, J. Opt. Soc. Am. B21, 1044, 2004.

32 K. Kasai and C. Fabre, Patent No.: US 6,433,918, 2002.

33 K. Kasai and C. Fabre, Japan Patent 3385328, 2003.

34 K. Hayasaka, Y. Zhang, and K. Kasai, Opt. Express 12, 3567, 2004.
35 K. Hayasaka, Y. Zhang, and K. Kasai, Opt. Lett. 29, 1665, 2004.
36 Y. Zhang, H. Su, C. Xie, and K. Peng, Phys. Lett. A 259, 171, 1999.
37 Y. Zhang, H. Wang, X. Li, J. Jing, C. Xie, and K. Peng, Phys. Rev. A 62, 023813, 2000.
38 K. Peng, Q. Pan, X. Li, J. Jing, J. Zhang, and C. Xie, Proc.7th Int. Conf. on Squeezed States and Uncertainty Relations, Boston, 2001. Available at http://www.physics.umd.edu/rgroups/ep/yskim/boston/boston.html
39 Y. Zhang, K. Kasai, and M. Watanabe, Phys. Lett. A 297, 29, 2002.
40 Y. Zhang, K. Kasai, and M. Watanabe, Eur. Phys. J. D 21, 361, 2002.

KASAI Katsuyuki

Senior Researcher, Quantum Information Technology Group, Kansai Advanced Research Center, Basic and Advanced Research Department

Quantum Optics

***ZHANG Yun**, Ph. D.*

Expert Researcher, Quantum Information Technology Group, Kansai Advanced Research Center, Basic and Advanced Research Department

Quantum Optics

***SASAKI Masahide**, Ph. D.*

Leader, Quantum Information Technology Group, Basic and Advanced Research Department

Quantum Information Theory